

Session MP60S-2

Mardi 17 mai 2022 de 17h40 à 18h10

Poster 19 à Poster 37



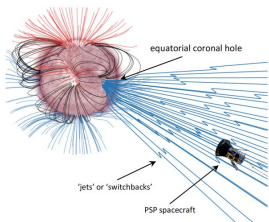
POSTER 19

Comparing Switchbacks formation mechanisms using
2.5D and 3D MHD simulations

Bahaeddine GANNOUNI

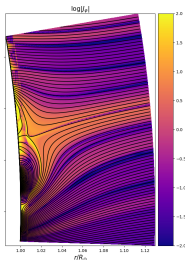


Origins of Magnetic Switchbacks



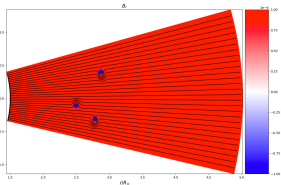
- Detected in solar wind unipolar region
- High Alfvénicity

Generation of Switchbacks



Simulation 2.5D MHD simulation
of emerging Pseudostreamer and reconnection

Propagation of Switchbacks



Switchbacks journey to PSp
and Solar Orbiter

POSTER 20

BibHelioTech

Vincent GÉNOT



POSTER 21

Solar Wind Plasma Properties During Ortho-Parker IMF Conditions and Associated Magnetosheath Mirror Instability Response

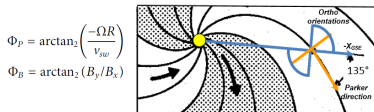
Vincent GÉNOT



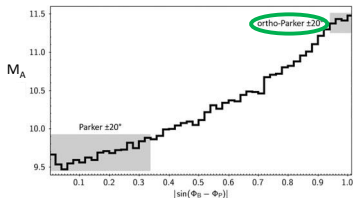
Solar Wind Plasma Properties During Ortho-Parker IMF Conditions and Associated Magnetosheath Mirror Instability Response

V. Génot & B. Lavraud

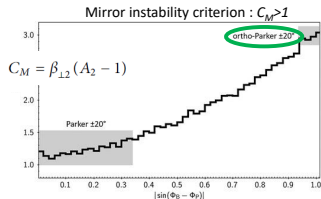
<https://doi.org/10.3389/fspas.2021.710851>



10 years of solar wind data



Rankine-Hugoniot analytical relations at the shock give beta and anisotropy in the downstream magnetosheath



Next step: use a large magnetosheath dataset to obtain the mirror threshold distribution in the whole sheath
 → preliminary result / come and see the poster !

POSTER 22

Magnetopause and bow shock models with machine learning

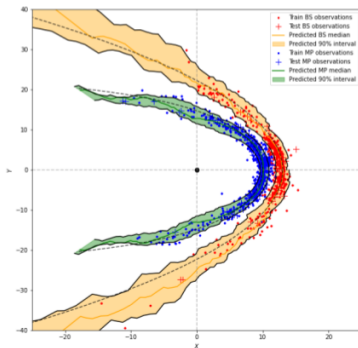
Ambre GHISALBERTI



New Magnetopause and Bow Shock models with machine learning

Existing analytical models :

- **Bow shock** : Jelinek et al., 2012; Jerab et al., 2005; Formisano et al., 1979.
- **Magnetopause** : Shue et al., 1997; Shue et al., 1998; Lin et al., 2010; Liu et al., 2015; Jelinek et al., 2012; Nguyen et al., 2021



They make different assumptions on symmetries, on the non correlation between features, etc.

→ We want to make a Gradient Boosting Regression model of the boundaries in order not to make those assumptions.

Ambre Ghisalberti, B. Michotte de Welle, N. Aunai, G. Nguyen



POSTER 23

Exploiting a catalogue of triangulated shock waves to study

Manon JARRY

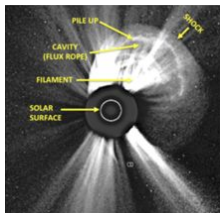


Exploiting a catalog of triangulated shock waves to study their kinematics and their roles in the acceleration of SEPs

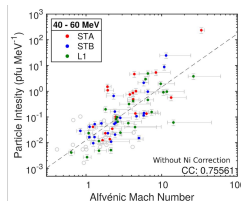
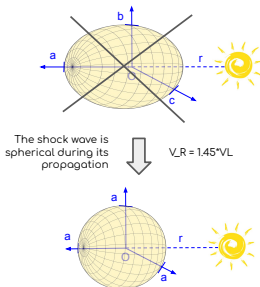


Manon Jarry, Alexis Rouillard, Illya Plotnikov, Athanasios Kouloumvakos

IRAP, CNRS, Université Toulouse III-Paul Sabatier, Toulouse, France



White light image of a Coronal Mass Ejection (CME) with a shock



Kouloumvakos et al. (2021), Particles intensity as a function of the Alfvénic Mach Number for one event

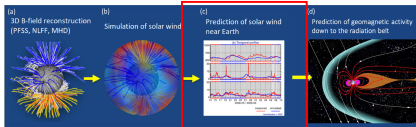
POSTER 24

Energy conversion through various channels in turbulent plasmas induced by the Kelvin-Helmholtz instability at the Earth's magnetopause

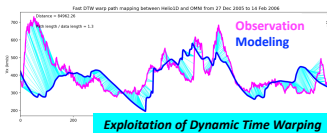
Rungployphan KIEOKAEW



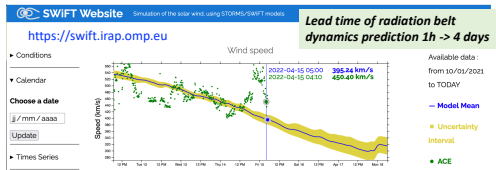
Pipeline for prediction of radiation belt environmental indicator



Modeling of solar wind stream interaction regions



Prototype pipeline for solar wind forecasting



This project has received funding from the European Union's [Horizon 2020 research and innovation programme](#) under grant agreement No 870437.

POSTER 25

Imagerie de la magnétosphère par rayons X :
simulations numériques en soutien à la mission SMILE

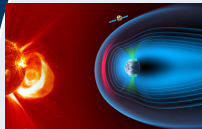
Dimitra KOUTROUMPA



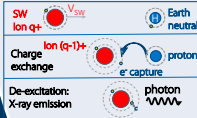
Solar wind charge exchange X-ray imaging of the magnetosphere: comparison of the MHD and test-particle approaches

D. Koutroumpa (LATMOS), R. Modolo (LATMOS), H. Connor (NASA-GSFC), S. Sembay (U. Leicester) & Y. Tkachenko (LERMA)

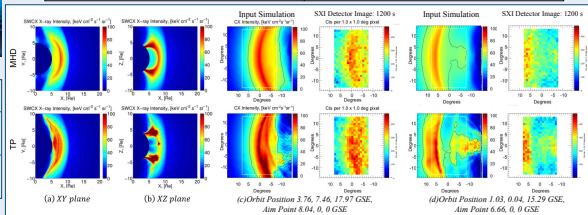
SMILE mission to observe the Sun-Earth Magnetosphere system in soft X-rays and UV.



Soft X-ray emission mechanism



MHD	Test-Particle (TP)
Single-fluid MHD description, no separate ion calculation	TP run for each ion species emissivity $Q_{TP}^{X^{q+}} \propto \text{col. probability}$
Self-computed E&B fields (solar & planetary origin)	Requires external E&B field input
Compound C.S. $\alpha_H = \sum_{X^{q+}, E} \alpha_{X^{q+}} Y_{X^{q+}, E}(E) \left[\frac{X^{q+}}{p} \right]$ proton bulk & thermal velocities	Individual ion C.S. ion velocities from Maxwellians
Total Emissivity: $Q_{MHD} = \alpha n_H n_p v_p$	Total Emissivity: $Q_{TP} = \sum_{X^{q+}, E} Q_{TP}^{X^{q+}} Y_{X^{q+}, E}(E) \left[\frac{X^{q+}}{p} \right]$



Adapted from Tkachenko et al. 2021, SF2A Proceedings
 This work is supported by CNES.



POSTER 26

First detection of the magnetic component of a radio wave emitted by the Sun

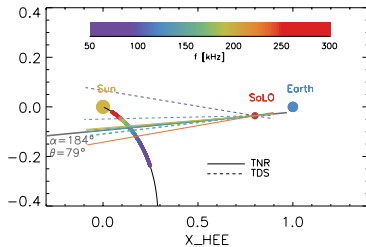
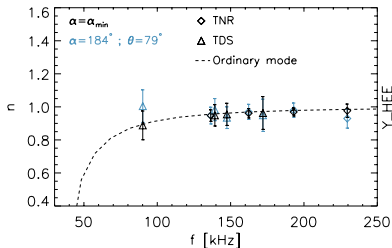
Matthieu KRETZSCHMAR



1st detection of the magnetic component of a solar radio wave during a type III radio burst

M. Kretzschmar and the RPW team

- Type III burst always observed with electric field only
- 1st detection of the magnetic component by SoLo/RPW
- ➔ Determination of the refractive index n and the wave vector k



POSTER 10

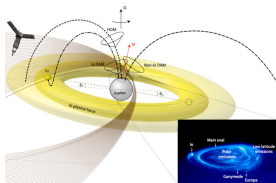
Étude des radiosources aurorales de Jupiter grâce à la sonde Juno

Briec COLLET



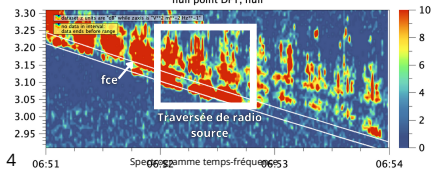
Etude in situ des traversées de sources radio joviennes aurorales

Brieuc Collet, Laurent Lamy, Corentin Louis, Philippe Zarka

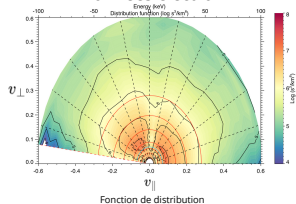


Données radio

Waves: 7 MHz Electric Waveforms null point DFT, null



Données electron



POSTER 29

Analyse multi-échelle d une couche de courant associée à un écoulement rapide pendant un sous-orage détecté par MMS

Olivier LE CONTEL





cnrs



Multiscale analysis of a current sheet embedded in a fast earthward flow during a substorm event detected by MMS

O. Le Contel, A. Retinò, A. Alexandrova, R. Nakamura, S. Alqeeq, T. Chust, L. Mirioni, F. Catapano, C. Jacquey, S. Toledo, J. Stawarz, K. A. Goodrich, D. J. Gershman, S. A. Fuselier, J. Mukherjee, N. Ahmadi, D. Graham, M. R. Argall, D. Fischer, S. Huang, J. L. Burch, R. B. Torbert, B. J. Giles, P.-A. Lindqvist, R. E. Ergun, Y. Khotyaintsev, F. D. Wilder, D. L. Turner, I. J. Cohen, H. Wei, R. J. Strangeway, K. R. Bromund, F. Plaschke

Poster 29, PNST, Marseille, 16-20 Mai 2022



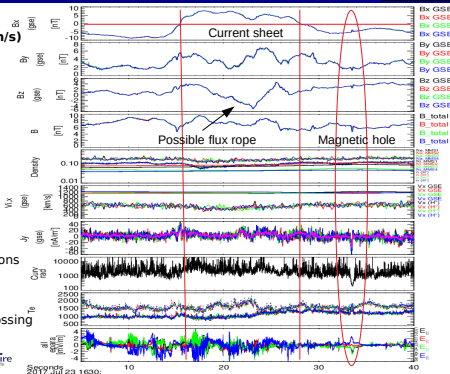
Corrugated ion scale CS detected during a fast earthward flow ($V_x \sim 500$ (FPI)-1200 (HPCA) km/s)

- with guide field $B_M/BL \sim 0.5$
- $N \sim 0.1$ p/cm³
- $J_y \sim J_{I_e} \sim 50$ nA/m²
- Curvature radius ~ 1000 km $\sim \pi$
- Parallel E fields related to electrostatic solitary waves (electron holes) associated with $T_{1,e} > T_{2,e}$
- Small dissipation $\mathbf{J} \cdot \mathbf{E} < 0.1$ nW/m³
- Possible « electron-only » reconnection signature

Possible flux rope (Bipolar Bz with Max By)
Not discussed in the poster

Electron scale magnetic hole

- Out of equator and associated with trapped hot electrons
- Large J_y up to -60 nA/m²
- Smaller curvature radius ~ 200 km $\sim 10\pi$
- $T_{1,e} > T_{2,e}$ but embedded in a plasma with $T_{1,e}/T_{2,e} < 1$
- Dissipation $\mathbf{J} \cdot \mathbf{E} \sim 0.15$ nW/m³ larger than at the CS crossing



SORBONNE université
UNIVERSITÉ PARIS-SACLAY



POSTER 30

E-SWAN, l'organisation de la météorologie de l'espace en Europe

Jean LILENSTEN

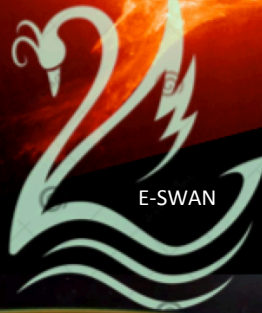


Welcome to E-SWAN

The European Space Weather and Space Climate Association (E-SWAN) is an international non-profit association established in 2022.

<https://eswan.eu/>

European Space Weather and Space Climate Association



To unite, sustain, and develop
Space Weather and Space
Climate activities in Europe

POSTER 31

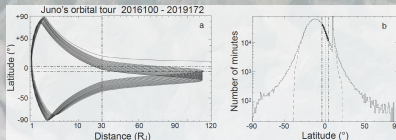
Latitudinal beaming of Jupiter's radio emissions from Juno/Waves flux density measurements

Corentin LOUIS

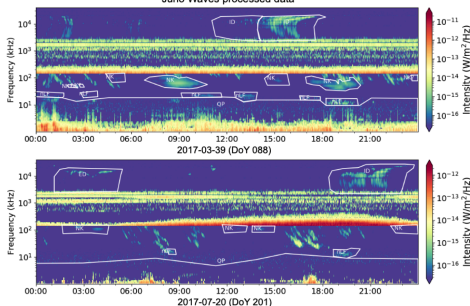


Aim: Constraint the Jovian radio emissions visibility

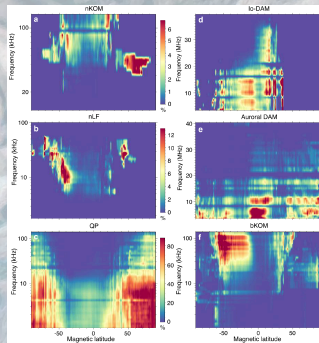
- **Calibration** of Juno radio observations
- **Catalogue** of Jovian radio emissions as observed by Juno
- First **latitudinal distribution** of Jovian radio emission, split by component
- First-order **interpretations**? Come and see my poster (and Adam Boudouma's)!



Juno Waves processed data



Background: Image of Jupiter's clouds [Juno Cam]



POSTER 32

Modeling the variability of Martian O^+ ions escape
due to Solar Wind forcing

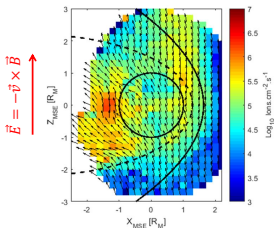
Ronan MODOLO





Modeling the variability of Martian O⁺ ions escape due to Solar Wind forcing R.Modolo et al – Poster # 32

MAVEN observed a **widespread spatial distribution of O⁺ ion fluxes** in the **Martian wake** and in the Northern MSE hemisphere (**plume**) => escaping ions



Simulation **diagnostic along the MAVEN trajectory** (in MSE) and projected in the XZ_{MSE} plane => Simulation emphasizes **two distinct escape channels** for O⁺ ions

Simulation results are valid for a given condition (upstream SW, local time, ...) while MAVEN results incorporate many different conditions

Investigation of parameters which affect the Solar wind – Mars interaction :

- Crustal Field locations
 - Solar wind density
 - Solar wind speed
 - IMF magnitude
 - θ_{VB}
 - Planet obliquity, EUV,
- Change P_{dyn}
- Change $\vec{E} = -\vec{v} \times \vec{B}$

POSTER 33

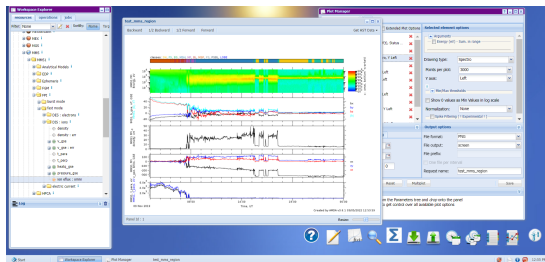
CDPP/AMDA, une base de données et un outil
d'analyse en ligne pour les données plasma
héliosphériques et planétaires

Benjamin RENARD



CDPP/AMDA, une base de données et un outil d'analyse en ligne pour les données plasma héliosphériques et planétaires

B. Renard, N. André, C. Jacquey, V. Génot, M. Bouchemit, A. Schulz, E. Budnik, N. Dufourg, I. Plotnikov et al.



- Accès à plus de **800 jeux de données** hétérogènes
- Accès à des **bases distantes** (CDAWeb, bases de simulation du LATMOS, FMI)
- **Edition de paramètres** à partir d'une expression mathématique
- **Tracé** des données
- **Téléchargement** des données
- **Recherche conditionnelle** sur les données
- **Statistiques** sur les données
- Edition / manipulation de **tables d'événement** et de **catalogues**
- **Interopérable** (EPN-TAP, SAMP, HAPI)
- Prédiction **Machine Learning**



<http://amda.cdpp.eu>

PNST : colloque scientifique Marseille, 16-20 mai 2022 – Thème 1 : Simulations et outils numériques - sciencesconf.org/pnst-2022:399972

POSTER 34

Mesure des vitesses photosphériques solaires via le suivi de structures cohérentes (granules)

Thierry ROUDIER



Coherent Structure Tracking (CST)

Roudier, Th.(1) Chane-Yook, M. (2), Rincon, F. (1), Rieutord, M. (1) and Malherbe, J.M. (3)
 (1) IRAP Toulouse (2) IAS Orsay (3) LESIA (Meudon)

Données du satellite HMI/SDO : Intensité et Doppler (45s.)
Suivi de 3 000 000 granules durant 30 min ⇒ **Vx and Vy et + Doppler (km/s)**
Résolution 2.5 Mm ⇒ **Vr Vθ Vφ**

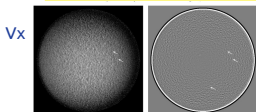


Fig. 7. Left: V_x component from the four exposures, spatial resolution 2.5 Mm. Arrows indicate the location of approximately 3000 dots on the Doppler map.

Fig. 8. Right: V_y component from the four exposures. When the solar granules have been selected, arrows indicate the location of approximately 3000 dots.

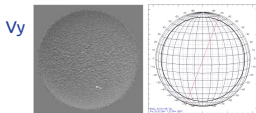


Fig. 9. Left: V_x component from the four exposures, spatial resolution 2.5 Mm. Arrows indicate the location of approximately 3000 dots on the Doppler map.

Fig. 10. Grid when the dark circle indicates the limit of the visibility of the heliographic velocity measurement.

V Doppler

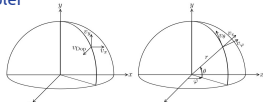


Fig. 10. Coordinate systems used throughout this paper: velocity components in the sky plane v_x and v_y and the line of sight v_z (left); velocity components on the solar surface v_r , v_θ , v_ϕ (right).



$uh = (V\theta, V\phi)$

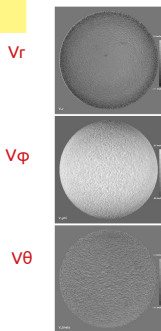
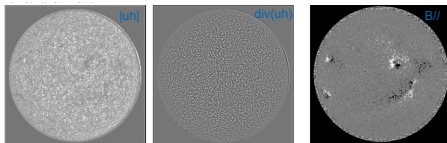


Fig. 12. v_r (left), v_θ (middle), v_ϕ (right) for the three-hour sequence August 30, 2011.

θ =latitude
 ϕ =longitude

Les codes CST et sa documentation sont disponibles sur le site de MEDOC
<https://idoc.ias.u-psud.fr/MEDOC/CST%20codes>

PNST 2022

POSTER 35

A 2D Self-consistent Sub-critical shock wave :
analysis of the shock front dynamics and its
associated ion and electron foreshocks

Philippe SAVOINI



Philippe Savoini¹ and Bertrand Lembège²

(1) LPP et (2) LATMOS

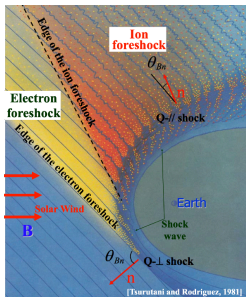
Poster n°35

Motivations:

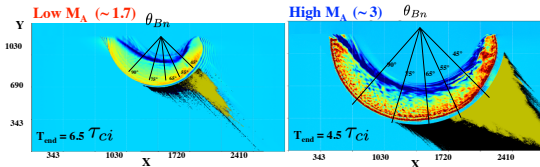
a) Most previous works dedicated to High M_A shock (both experi./numeri. Simul)b) Evidence of Low M_A shock waves (experim.) raise up several questions:→ Persistence of associated foreshocks for low M_A ?→ If foreshocks persist, what is the impact of a varying M_A :

- on the bow shock profiles / time dynamics ??

- on the spatial (radial & angular) extension of each foreshock ??

- on the local distribution functions $f_{i,e}(v)$ contributing to each foreshock→ here we focus on local $f_i(v)$ (GPB versus FAB) (preliminary results..... at the poster)

Present 2D PIC simulation results



POSTER 36

Python tools for CDDP/AMDA and Machine Learning

Alexandre SCHULZ

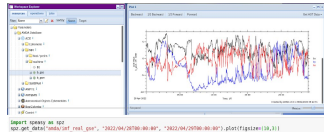


Python tools for CDP/AMDA and Machine Learning

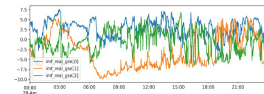
Alexandre Schulz – CDP/IRAP

Speasy: Space Physics made EASY:

- GitHub : <https://github.com/SciQLop/speasy>
- Downloading space physics datasets from AMDA, CDAWeb and SSCWeb
- Supports Time-series, Timetables, Catalogs
- Jupyter notebook integration

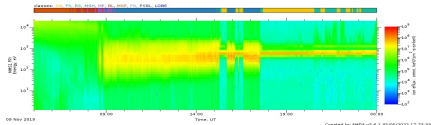


```
!pip install ORF
!or_get_data('speasy/inf_inf', "2022/04/20T00:00:00", "2022/04/20T00:00:00").plot(figsize=(10,11))
```



Orchestra: Machine Learning

- GitHub : <https://github.com/cdppirap/orchestra>
- Prediction and training of models, execution managed with **Docker**



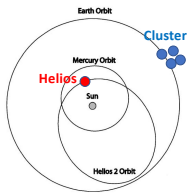
POSTER 37

Dissipation range of solar wind turbulence

Olga ALEXANDROVA

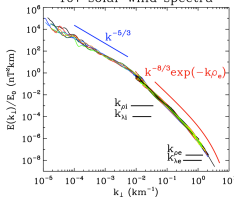


Dissipation range of solar wind turbulence



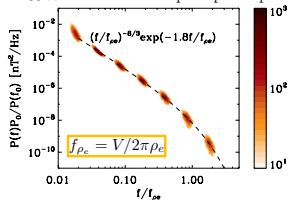
[Alexandrova et al. 2012]

107 solar wind spectra



[Alexandrova, Jagarlamudi et al. 2021]

3344 normalised and superimposed spectra



$$E(k) = Ak^{-8/3} \exp(-k\ell_d), \quad \ell_d = 1.8\rho_e$$

- Spectral rolling: signature of turbulence dissipation
- The dissipative scale ℓ_d : **electron Larmor radius** (~ 300 m at 0.3 AU and ~ 1 km at 1 AU) $\rho_e = \frac{V_{th,e}}{2\pi f_{ce}}$
- The same spectral shape is observed for different plasma parameters and at different distances from the Sun, 0.3-0.9 AU (Helios) and 1 AU (Cluster) => **toward the generality of the phenomena ?!**
- ...and what about Parker Solar Probe and Solar Orbiter observations ?